Food Research International 174 (2023) 113644

Contents lists available at ScienceDirect

Food Research International

journal homepage: www.elsevier.com/locate/foodres

Untargeted metabolomics provide new insights into the implication of *Lactobacillus helveticus* strains isolated from natural whey starter in methylglyoxal-mediated browning

Sofia Galimberti [a,1], Gabriele Rocchetti [b,1], Francesca Di Rico [c], Chiara Rossetti [a], Alessandra Fontana [a], Luigi Lucini [c], Maria Luisa Callegari [a,*]

[a] Department for Sustainable Food Process, Università Cattolica del Sacro Cuore, Via Bissolati 74, 26100 Cremona, Italy
[b] Department of Animal Science, Food and Nutrition, Università Cattolica del Sacro Cuore, Via Emilia Parmense 84, 29122 Piacenza, Italy
[c] Department for Sustainable Food Process, Università Cattolica del Sacro Cuore, Via Emilia Parmense 84, 29122 Piacenza, Italy

ARTICLE INFO

Keywords:
Grana-like cheese
Maillard reaction
Starter lactic acid bacteria
UHPLC-HRMS
Pyrazines

ABSTRACT

Hard cheeses may occasionally show a brown discolouration during ripening due to multifactorial phenomena that involve bacteria and give rise to pyrazines arising from methylglyoxal. The present work aimed at developing a novel approach to investigate the role of natural starters in browning. To this object, 11 strains of *L. helveticus* were incubated in a medium containing 10 % rennet casein dissolved in whey, and then growth was monitored by measuring pH and number of genomes/mL. Browning was assessed through CIELab analysis, methylglyoxal production was determined by targeted mass spectrometry, and untargeted metabolomics was used to extrapolate marker compounds associated with browning discoloration. The medium allowed the growth of all the strains tested and differences in colour were observed, especially for strain A7 (ΔE^* value 15.92 ± 0.27). Noteworthy, this strain was also the higher producer of methylglyoxal (2.44 μg/mL). Metabolomics highlighted pyrazines and β-carboline compounds as markers of browning at 42 °C and 16 °C, respectively. Moreover, multivariate statistics pointed out differences in free amino acids and oligopeptides linked to proteolysis, while 1,2-propanediol and S-Lactoylglutathione suggested specific detoxification route in methylglyoxal-producing strains. Our model allowed detecting differences in browning amid strains, paving the way towards the study of individual *L. helveticus* strains to identify the variables leading to discoloration or to study the interaction between different strains in natural whey starters.

1. Introduction

The development of brown pigmentation can occur during the latter ripening and storage periods of hard cheese, leading to the economic depreciation (Gandhi et al., 2019). This defect impacts on the product's appearance, texture and flavour (Yann et al., 2005). Unlike the typical Maillard reactions, the browning reactions in hard cheeses can proceed at relatively low temperatures and reduced sugars are not required (Gandhi et al., 2018).

In cheese, brown pigmentation is linked to the microbial production of methylglyoxal (MG) (Zheng et al., 2021). MG can be produced by several bacteria via the conversion of dihydroxyacetone phosphate (DHAP) derived from glycolysis (Divine and Rankin, 2013; Gandhi et al., 2019), to be excreted into the growth medium (Ackerman et al., 1974; Russell, 1993). This natural metabolite is extremely cytotoxic and MG-tolerant bacteria possess several ways for its detoxification (Ferguson et al., 1998, Lee and Park, 2017, Gandhi et al., 2018). The excess of methylglyoxal produced may react with the amine groups of proteins, peptides, and free amino acids through the protein–diketone reaction and produces brown pigmentation and characteristic volatiles (Divine et al., 2012; Divine and Rankin, 2013; Hatti-Kaul et al., 2018). Many works are available in scientific literature dealing with the Maillard reaction (This, 2015; Li et al., 2022), although non-enzymatic browning has been less investigated (Zheng et al., 2021). Divine et al. (2012) described the importance of pyrazines, known as key flavour compounds in many hard-cooked cheeses, to modulate the browning process in

* Corresponding author.
E-mail address: marialuisa.callegari@unicatt.it (M.L. Callegari).
[1] These authors contributed equally to this work.

https://doi.org/10.1016/j.foodres.2023.113644
Received 2 August 2023; Received in revised form 23 October 2023; Accepted 24 October 2023
Available online 26 October 2023

Parmesan cheese. These compounds result from the spontaneous condensation of aminoacetone derived from Strecker degradation of amino acids with MG. Accordingly, the production of pyrazines can be mainly influenced by free amino acids and peptides, as highlighted by Scalone et al. (2015). Bacterial production of MG can promotes the formation of late reaction compounds typical of the Maillard reaction, such as β-carbolines and melanoidin, even at relatively low temperatures (Gandhi et al., 2019). However, to date, no works based on comprehensive chemical profiling approaches to evaluate the processes involved in browning are available in the literature.

The browning defect has been poorly explored also from a microbiological point of view. The production of Grana cheese involves the use of a natural starter composed mainly of starter lactic acid bacteria (SLAB) and non-starter lactic acid bacteria (NSLAB), which come from raw milk (Giraffa, 2021; Neviani et al., 2013). The natural starter bacteria are responsible for the rapid acidification of curd in the early stages of cheese production. After that, when the growth conditions become limiting, cells go into autolysis. At this stage, NSLAB replace the natural starter bacteria and contribute to ripening (Neviani et al., 2013). Both LAB populations may produce MG and can potentially contribute to browning, including *L. helveticus* that is predominant species in natural whey starter. Strains belonging to *L. helveticus* species have been described as moderate producers of MG (Divine and Rankin, 2013) and for this reason they are not considered involved in browning, as high levels are required to achieve discoloration (McDonald, 1992). Nevertheless, Bottazzi et al. (2000), in a cheese-making model, obtained a discoloration in Grana cheese using a single strain of *L. helveticus* (strain CNBL1386) as a starter culture.

Given the key role of *L. helveticus* in the production of hard cheeses, we believe that further studies on the implication of this species in browning are needed. The main objective of the work was to develop a novel approach to investigate the role of natural starters in browning, and to provide biochemical insights into the processes leading to discoloration.

2. Materials and methods

2.1. Bacterial isolation, identification and typing

Natural whey cultures of Grana-like cheese were collected from one dairy plant at different periods of the year. Ten-fold serial dilutions were spread onto a whey agar medium supplemented with 2 % yeast extract. Whey based media normally replaced synthetic media for growing the strains contained in natural whey starters since the latter do not support their growth (Miragoli et al., 2020). Plates were anaerobically incubated at 42 °C for 48 h. Colonies were picked up and serially streaked on the same medium to obtain pure cultures.

Bacterial DNAs were extracted from colonies using the microLYSIS® DNA release buffer (Clent Life Science, Stourbridge, UK) as indicated by manufacturer's instructions. To identify strains, the extracted DNAs were used as a target in PCR reactions with primers designed on the phenylalanine-tRNA synthetase (*pheS*) gene sequence according to the protocol described by Moser et al (2017) (Moser et al., 2017a). Moreover, the typing of strains was obtained by mean of the PCR-DGGE analysis following the protocol described by Miragoli et al. (2020).

Briefly, bacterial DNAs were used to amplify the discriminant region of S-layer gene using the three primer pairs targeting *slpH* group 1, *slpH* group 2, and *slpH* group 3. Amplicons were analyzed by the PCR-DGGE using the INGENYphor 2 × 2 System (INGENYphor, Goes, The Netherlands). Amplicons from *slpH* group 2 and *slpH* group 3 strains were run respectively in a 6 % and 8 % (w/v) polyacrylamide gel (37.5/1, acrylamide/bis-acrylamide), with 30–40 % denaturing agents (urea and formamide). Electrophoresis for both gels was performed at 100 V for 18 h at 60 °C.

2.2. Development of a suitable medium for selecting browning-producer strains

2.2.1. Development of medium and preliminary tests using L. helveticus CNBL 1386

A series of preliminary tests was carried out considered *L. helveticus* CNBL 1386 used by Bottazzi et al. (2000). This strain is still available in the Collezione Nazionale Batteri Lattici (CNBL) (Università Cattolica del Sacro Cuore, Piacenza, Italy). In these tests, CNBL 1386 strain was chosen as a positive control since already described as capable of browning in Grana cheese. Food grade rennet casein powder (10 %) (S. C.A., Fiorenzuola, Piacenza, Italy) was resuspended in whey to obtain the rennet casein whey medium (RCWM). The whey used for medium preparation was filtered as previously described by Cocconcelli et al. (1997). The casein suspension was heated in the microwave oven for 3 min at 400 W (temperature reached approximately 100 °C) and then the medium was kept mixed and distributed in sterile tubes. A series of preliminary tests was carried out by inoculating the tubes with our isolates and incubating them at 42 °C until a change of colour appeared. In all preliminary tests, the inoculum used was an overnight culture in whey. In all these tests, we used inoculums independent of previous one. Moreover, to evaluate the importance of the inoculum on the color changes serial dilution of overnight culture were used. Then we inoculated RCWM with 1 % of an overnight culture of strain CNBL 1386 (10^7 CFU/mL), and its dilution 1/10 and 1/100. Incubation was carried out at 42 °C as previously described.

In each test the incubation was at 42 °C and colour changes was monitored periodically (each 24 h). These preliminary tests were repeated several times and for this reason, we set at 72 h the duration of incubation. In order to monitor the evolution of colour changes after active growth of the strains, we decided to apply an additional incubation at 16 °C.

2.2.2. Selection of browning-producer strains

Once the system was in place, we start with an assay taking in consideration only our 11 strains. The overnight culture of our isolates, grown in whey medium, was used as an inoculum for two sets of RCWM tubes, which were then incubated at 42 °C for 72 h. In parallel, the same procedure was repeated in tubes containing whey (i.e., representing our control), considering that in dairy plants these strains are traditionally propagated in this medium. Then we consider whey the ideal medium for their growth. At the end of the incubation, the first series of tubes were used for the microbiological and colorimetric analysis. After that, the second series of cultures were placed at 16 °C for 72 h to evaluate further colour changes via colorimetric measurements.

2.3. Quantification of L. helveticus strains by real time-PCR

Real time-PCRs were performed to quantify the number of bacterial cells in RCWM and whey after the incubation at 42 °C for 72 h. This approach was preferred to the culture-dependent techniques due to their limitation in assessing the number of viable cells after a long incubation time. In fact, during preliminary tests, under our conditions, plate counts indicated that some strains reached the stationary phase after 48 h of incubation while, at 72 h, the number of viable cells was reduced by an average of one log. Then, the data obtained from the RCWM cultures were compared to those of the whey cultures by mean of real time-PCR.

The bacterial DNAs from these samples (500 μL) were extracted using the Maxwell® 16 Tissue DNA Purification Kit and the Maxwell® 16 Instrument (Promega, Madison, WI, USA). The real time-PCR reactions were performed in triplicate using 250 nM of LbhelvF1 and LbhelvR1 primers, already used for strain identification (Moser et al., 2017a). All analyses were conducted in a LightCycler ®480 Instrument II (Roche Life Science, Mannheim, Germany) using a KAPA SYBR® FAST qPCR Master Mix (2X) Kit (KAPA Biosystems, USA). Standard curves were generated using the DNA of *L. helveticus* ATCC15009™ strain

(Type strain from American Type Culture Collection) as a reference. The thermal cycle conditions were the following: a denaturation step at 95 °C for 3 min followed by 40 cycles at 95 °C for 10 s, 60 °C for 50 s. Finally, melting curves of the amplicons were obtained by monitoring fluorescence from 65 to 97 °C, with temperature increments of 0.2 °C. Results were obtained as gene copy number/mL of sample. Our real time- PCR results will be expressed as genome number/mL, as the target gene used for its quantification is present in only one copy in the genome of *L. helveticus*.

2.4. Colour measurement evaluation

The colour measurement of the samples was carried out using Colorflex EZ spectrophotocolorimeter (Hunterlab, Reston, Virginia). To evaluate the colour changes of samples after both incubations, the content of the tubes was placed into petri dishes (Falcon 3001, Becton Dickinson). Colour was measured in triplicate for each sample, and the results were expressed according to CIEL*a*b*colour space using a D65 illuminant source and a 10° viewing angle.

The colour was measured through three-dimensional colour diagram (L*, a* and b*), where: L* indicates lightness (L* = 0 (black), L* = 100 (white), a* indicates (−a* = greenness, +a* = redness) and b* chromaticity indicates (−b* = blueness, +b* = yellowness). The Chroma (C*) and hue (h) were also calculated as follow: $C^* = [(a^*)^2+(b^*)^2]^{1/2}$ h = arctan (b/a) (Hernández et al., 2016).

The Chroma (C*) refers to the saturation and the purity of a colour: a high C* is related to a more vivid colour, and its values vary over a range of colours from black to grey. The hue angle (h) represents the amplitude of the angle formed by taking the ± a* axis as × and it is characterized as follows: 0° for redness, 90° for yellow, 180° for green, and 270° for blue.

Total Colour difference (ΔE*) was calculated according to the following equations:

$\Delta E^* = [(\Delta L)^2+(\Delta a)^2+(\Delta b)^2]^{1/2}$, in which $\Delta L^* = L_1 - L_2$; $\Delta a^* = a_1 - a_2$; $\Delta b^* = b_1 - b_2$ (Biró et al., 2019).

2.5. Targeted quantification of methylglyoxal by UHPLC-MS/MS

The derivatization of methylglyoxal (MG) for targeted UHPLC-MS/MS analysis was carried out following the protocol previously described by Fritzsche et al. (2018), based on the utilization of 4-methoxy-*o*-phenylenediamine dihydrochloride (4-PDA) as derivatization agent, with few modifications. Briefly, a stock solution in water of 20 mM MG (from BioVision, Milpitas, USA) was used to prepare a calibration curve, considering a range 0.9–250 μg/L, while 4-PDA was prepared in methanol at the final concentration of 10 mM. For the derivatization reaction, 500 μL of MG or experimental samples (RCWM and WM) were allowed to react with 500 μL of 20 % acetonitrile (pH = 4) and 25 μL of 4-PDA 10 mM. The reaction was done in 2 mL-eppendorf tubes for 2 h in dark conditions, under continuous agitation. Each sample was centrifuged for 10 min at 13,000 xg, filtered through 0.20 μm regenerated cellulose syringe-filters (Sartorius Minisart™) and then transferred in UHPLC vials for instrumental analyses.

The targeted analysis was done using a Q Exactive™ Focus Hybrid Quadrupole-Orbitrap Mass Spectrometer (Thermo Scientific, Waltham, MA, USA) coupled to a Vanquish ultra-high-pressure liquid chromatography (UHPLC) pump and equipped with heated electrospray ionization (HESI)-II probe (Thermo Scientific, USA). The chromatographic separation was based on a water (A) and acetonitrile (B) (both LC-MS grade, from Sigma-Aldrich, Milan, Italy) gradient elution (20–70 % acetonitrile in 28 min), using an Eclipse Plus (from Agilent) C18 column (100 × 4.6 mm, 2.7 μm). Formic acid 0.1 % (v/v) was used as phase modifier and added to both A and B. The flow rate was 200 μL/min, while the injection volume was 0.6 μL, using a full scan MS analysis (50–500 *m/z* range) coupled with a parallel reaction monitoring (PRM) mode. The analysis was done considering a positive ionization and a mass resolution of 35,000 at *m/z* 200, with an automatic gain control (AGC) target value of 1×10^5, maximum injection time (IT) of 100 ms, and isolation window of 2.0 *m/z*. For the PRM analysis, the inclusion list consisted of the protonated $[(M + H)^+]$ reaction product of MG, namely methoxy-2-methylquinoaxaline (parent ion; accurate mass: 175.0860; Fritzsche et al., 2018) that was fragmented using 20 eV as normalized collisional energy. Two representative product ions were targeted, namely 160.0628 *m/z* and 132.0680 *m/z* (supplementary table 4, data sheet a.). The XCalibur software was used for both data acquisition and processing, using the external calibration approach to achieve absolute quantification of MG in the studied samples (μg/mL, n = 3).

2.6. Untargeted metabolomics based on UHPLC-HRMS characterization of browning pigments

As far as the extraction step is concerned, 200 μL of each sample (RCWM and WM) were dissolved in 800 μL MeOH 80 % (acidified with 0.1 % formic acid) and then incubated 15 min in an ultrasonic bath, thus exploiting an ultrasound-assisted extraction (UAE). Thereafter, samples were centrifuged at 10,000 × *g* for 10 min at 4 °C, and the corresponding supernatants were filtered using cellulose syringe filters (0.2 μm) in vials and stored at −18 °C until instrumental analysis.

The untargeted metabolomics analysis was done using a Q Exactive™ Focus Hybrid Quadrupole-Orbitrap Mass Spectrometer (Thermo Scientific, Waltham, MA, USA) coupled to a Vanquish ultra-high-pressure liquid chromatography (UHPLC) pump and equipped with heated electrospray ionization (HESI)-II probe (Thermo Scientific, USA), as optimized in a previous work (Rocchetti et al., 2021). Briefly, the chromatographic separation was achieved under a water-acetonitrile (both LC-MS grade, from Sigma-Aldrich, Milan, Italy) gradient elution (from 6 up to 94 % acetonitrile in 35 min), using 0.1 % formic acid in both LC solvents and a Waters BEH C18 as separation column (100 × 2.1 mm, 1.7 μm). The flow rate was 200 μL/min (injecting 6 μL) and the analysis was done under a full scan MS mode (50–750 *m/z* range) according to a positive ionization, setting a mass resolution of 70,000 at *m/z* 200. The AGC target and the maximum IT parameters are reported elsewhere (Rocchetti et al., 2021). A pooled quality control (QC) sample was prepared and randomly analyzed in a data-dependent (Top N = 3) MS/MS mode, reducing the MS resolution to 17,500 at *m/z* 200, with an AGC target value of 1×10^5, maximum IT of 100 ms, and an isolation window of 2.0 *m/z*, respectively. The Top N ions were fragmented using typical collisional energy values (i.e., 10, 20, 40 eV). The HESI parameters are reported in a previous work from our research group (Rocchetti et al., 2021). The mass spectrometer was calibrated before each run using a Pierce™ positive ion calibration solution (Thermo Fisher Scientific, San Jose, CA, USA).

The collected.RAW data were further processed using the software MS-DIAL (version 4.70). The pre-processing steps consisted in automatic peak finding, retention time alignment, Lowess normalization, and annotation via spectral matching against the database FooDB version 1.0 (https://www.foodb.ca) were adopted. The mass range 50–750 *m/z* was searched for features with a minimum peak height of 10,000 cycles per second (cps). The MS and MS/MS mass tolerance for peak centroiding and features annotation was set to 0.05 and 0.1 Da, respectively. The annotation step was based on mass accuracy, isotopic pattern, and spectral matching, considering a level 2 of confidence in annotation (Blaženović et al., 2018). The selected identification criteria were used to calculate a total identification score. The total identification score cut off was > 50 %, considering the most common HESI + adducts (Rocchetti et al., 2021). Finally, gap filling (using the peak finder algorithm) was used to fill in missing peaks, considering a 5-ppm tolerance for *m/z* values.

2.7. Evaluation of the autolytic capacity of L. helveticus strains

The strains were grown in RCWM medium and incubated as previously described; 1 mL of bacterial suspension was collected at 24-hour

intervals while 100 μL were used for plate counting. Cells were removed by centrifugation (10,000 × g for 10 min) and subsequent filtration on 0.2 μm filters (VWR, Radnor, PA, USA) (Treimo et al., 2006). The cell-free samples were immediately frozen at −20 °C. These supernatants were purified and concentrate using the DNA Clean & Concentrator Kit (Zymo Research, Irvine, CA) following the manufacturer's instructions. The volume of supernatant purified was 200 μL for each sample while the final elution volume was 20 μL. The purified DNAs were used as targets in real time-PCR reactions with the same primers and conditions described in the previous sections. The same procedure was used for the control (medium incubated without inoculum).

2.8. Statistical analyses

The one-way analysis of variance (ANOVA; $p < 0.05$, Duncan's post-hoc test) was done using the software IBM PASW Statistics 26.0 (SPSS Inc.) to investigate significant differences in LAB counts, pH values and MG content. Concerning the colorimetric data, statistical differences were evaluated by ANOVA with Tukey's post-hoc testing at $p \leq 0.05$.

The multivariate statistical elaboration of metabolomics-based data was done using two different software, namely MetaboAnalyst 5.0 (Pang et al., 2021) and SIMCA 13 (Umetrics, Malmo, Sweden), according to the typical workflow for untargeted metabolomics-based experiments, previously described in Rocchetti et al. (2021). Overall, the data were normalized by the median, Log transformed, and Pareto scaled, following the normalization procedure on MetaboAnalyst. Both unsupervised and supervised multivariate statistics were carried out based on hierarchical clustering analysis, principal component analysis (PCA), and orthogonal projections to latent structures discriminant analysis (OPLS-DA), considering data from both the temperature conditions tested. In particular, the supervised OPLS-DA models were built considering the browning effect as sample grouping condition, as observed from the colorimetric assays (paragraph 2.4). Additionally, the OPLS-DA model validation parameters (goodness-of-fit R^2Y and goodness-of-prediction Q^2Y) were inspected. The importance of each metabolite for discrimination purposes was assessed through a VIP (variables importance in projection) selection method, considering as the minimum significant threshold VIP scores > 0.8 (Senizza et al., 2020). Furthermore, a Venn analysis was done using the online tool Venny 2.1 (https://bioinfogp.cnb.csic.es/tools/venny/index.html), to discern among the most significant and exclusive discriminant markers of both OPLS-DA prediction models built. Finally, considering the MG detoxification pathways previously described for LAB by Gandhi et al. (2018), we evaluated the significant variation of those metabolites directly or indirectly involved in the browning process using both a Volcano Plot analysis (built on the software Mass Profiler Professional B.12.06, from Agilent Technologies), i.e., combining one-way Anova ($p < 0.05$) and a Log_2 Fold-Change analysis, and a Receiver Operating Characteristics (ROC) approach (built on MetaboAnalyst 5.0). The metabolites considered were mainly glycolysis intermediates, pyrazines, Maillard reaction products, AGE, amino acids, peptides, furans, and furanones.

3. Results and discussion

3.1. Bacterial isolation

A series of whey samples were collected from a dairy plant in which sporadically browning discoloration was observed in Grana-like cheese products. From these samples, eleven strains of *L. helveticus* were isolated and identified. Based on nucleotide polymorphisms of S-layer gene, strains of *L. helveticus* were divided into three different groups (from 1 to 3) (Moser et al., 2017b). Later, three sets of primers targeting the *slpH* locus were used to discriminate strains based on the different migration in PCR-DGGE gels. According to the specific domains, strains were clustered into *slpH* group 1, *slpH* group 2, and *slpH* group 3 (Miragoli et al., 2020). According to PCR-DGGE analysis ten strains (A1, A7, A17, A23, A34, E7, E16, E28, E44 and E45) out of the total resulted belonging to *slpH* group 2 strains, whereas the remaining A10 strain to the *slpH* group 3. No strain was found to belong to *slpH* group 1 in accordance with a study that also analysed natural starter cultures of Grana Padano PDO cheese (Miragoli et al., 2020).

3.2. Utilization of RCWM to highlight browning producer strains

3.2.1. Microbiological evaluation

A specific medium is necessary to evaluate the potential of *L. helveticus* to induce browning. Such medium should be easy to prepare, constant in composition, guarantee the growth of the tested strains and highlight any colour variations. In a previous work, a Parmesan cheese extract medium (Gandhi et al., 2018) has been proven as effective in identifying the ability of lactobacilli to produce browning; however, its preparation can be elaborated and time-consuming. For this reason, we decided to develop a new medium. Nonetheless, considering that browning has often been associated with the presence of MG and final products of proteolytic activities, supplementation with casein in the assay medium was considered essential. Finally, we added 10 % rennet casein to the whey (pH approx. 6.2) and started preliminary tests.

Preliminary tests were conducted to assess the bacterial growth and optimal conditions for detecting discoloration. To this aim, the CNBL 1386 strain was used as positive control. According to our results, the composition of RCWM supported the growth of the CNBL 1386 strain, which reached 5×10^8 CFU/mL and pH 3.8 in 24 h of incubation at 42 °C. In addition, the influence of inoculum on staining was evaluated. Indeed, a 1 % inoculum with a culture containing 10^7 CFU/mL and the respective decimal dilutions (1/10, 1/100) did not change the intensity of the colour produced after incubation. This indicated that within a certain range of CFU/mL values, the inoculation is not a critical factor.

Based on these preliminary data and once defining the protocol conditions, all strains were tested three times in independent assays ($n = 3$). As reported in materials and methods, two incubation steps were applied. The former incubation was at 42 °C for 72 h, while the latter consisted in a first incubation at 42 °C for 72 h followed by a post-incubation at 16 °C for the same time. In the text, we will refer to the first step as "42 °C" and to the second step as a "16 °C". The bacterial population in the first incubation was actively growing and the compounds produced can be considered as the result of their metabolisms. In post-incubation at 16 °C, however, it can be assumed that the contribution of the metabolism is no longer of primary importance and variations in the medium may be essentially due to both compounds and/or enzymes accumulated in the previous phase or released during the second phase via the lysis of *L. helveticus* (resting) cells. The growth parameters evaluated after 72 h at 42 °C are presented in Table 1, in which the quantification of bacterial strains obtained by real time-PCR is reported. Overall, no significant differences were found between the pH values of the *L. helveticus* strains grown in RCWM *vs* WM, being on average 3.66 *vs* 3.79, respectively (p-value = 0.146), whereas a significantly higher ($p < 0.01$) number of genomes/mL was found in RCWM compared to WM, being on average 9.08 *vs* 8.30, respectively (Table 1).

3.2.2. Colour development and colorimetric analysis

In our preliminary tests, the incubation at 42 °C for 72 h caused the appearance of a brown discoloration for strain CNBL 1386 in agreement with the previous report of Bottazzi et al. (2000) without the demanding approach of cheese-making tests. The colorimetric analysis revealed the following coordinate (L* 71.42 ± 0.05; a* 1.15 ± 0.15; b* 15.14 ± 0.14) the calculated ΔE* value was 11.00 ± 0.16 indicating a visual difference compared to control. These results suggested that RCWM used in this experiment was suitable for highlighting the ability of this strain to cause browning.

Concerning our isolates, only the tube corresponding to the A7 strain showed a reddish colour after the first incubation step at 42 °C,

Table 1
pH values and log number of genomes/mL after incubation at 42 °C of *L. helveticus* strains in RCWM and WM. Results are expressed as mean values ± standard deviation (n = 3). We also report the statistical significance of pH and growth values when comparing *L. helveticus* strains grown in RCWM with those grown in WM, as revealed by one-way ANOVA. The last two columns of the table show the values of residual methylglyoxal (MG) production after incubation at 42 °C of *L. helveticus* strains grown in RCWM and WM. The results are presented as mean values (μg/mL) ± standard deviation. The superscript letters (a-i) within each column indicate significant differences as a result of the Duncan post-hoc test following one-way ANOVA ($p < 0.05$). nd = not detected. CTR: negative control tube (not inoculated).

Strain	pH RCWM	pH WM	Log number of genomes/mL RCWM	Log number of genomes/mL WM	MG μg/mL RCWM	MG μg/mL WM
A1	3.94 ± 0.06	3.72 ± 0.14	8.95 ± 0.02	8.67 ± 0.02	1.00 ± 0.03^{c}	0.63 ± 0.01 ^{g}
A7	3.75 ± 0.04	3.73 ± 0.04	8.63 ± 0.02	8.16 ± 0.00	2.44 ± 0.02^{i}	0.65 ± 0.00 ^{h}
A10	3.58 ± 0.01	3.50 ± 0.07	8.68 ± 0.02	7.89 ± 0.00	1.72 ± 0.02^{e}	0.09 ± 0.00^{d}
A17	3.59 ± 0.03	3.51 ± 0.02	9.49 ± 0.09	8.30 ± 0.00	1.97 ± 0.03 ^{g}	0.07 ± 0.00^{c}
A23	3.62 ± 0.03	4.14 ± 0.08	9.41 ± 0.01	8.53 ± 0.01	1.03 ± 0.02^{c}	0.83 ± 0.01^{j}
A34	3.59 ± 0.06	3.51 ± 0.03	9.18 ± 0.00	8.19 ± 0.00	1.41 ± 0.02^{d}	0.05 ± 0.00^{b}
E7	3.66 ± 0.08	3.80 ± 0.06	8.53 ± 0.02	8.09 ± 0.01	0.47 ± 0.00^{a}	0.02 ± 0.00^{a}
E16	3.94 ± 0.06	4.24 ± 0.16	8.82 ± 0.01	8.81 ± 0.01	1.89 ± 0.02 ^{g}	0.89 ± 0.02 ^{k}
E28	3.57 ± 0.19	3.89 ± 0.05	9.43 ± 0.02	8.25 ± 0.00	1.79 ± 0.03^{f}	0.44 ± 0.01^{f}
E44	3.55 ± 0.07	3.85 ± 0.02	9.93 ± 0.00	8.30 ± 0.01	0.86 ± 0.02^{b}	0.39 ± 0.00^{e}
E45	3.55 ± 0.03	3.89 ± 0.08	8.93 ± 0.01	8.18 ± 0.01	2.08 ± 0.03 ^{h}	0.69 ± 0.00^{i}
CTR	3.94 ± 0.06	nd	nd	nd	nd	nd
p-value RCWM *vs* WM	$p > 0.05$		$p < 0.01$			

compared to the other tubes that revealed a cream colour substrate (Fig. 1 A). The control tube, instead, appeared white. The evaluation of a 16 °C post-incubation step was intended to account also for the slowest reactions involved in colour development, as it has been reported to contribute towards browning defect (Gandhi et al., 2018). Indeed, it is well known that the browning defect is due to slow chemical reactions occurring at low temperatures. Moreover, this temperature is traditionally used for Grana cheese ripening. After this incubation, a colour darkening was visible for the A10 strain, even if some changes were detectable also for the others (Fig. 1 B). For example, for the A7 strain, the red coloration resulted in being lighter than before. Some differences could be easily detected during this first visual examination of the tubes, while others were less obvious. Colorimetric measurements were carried out to evaluate the colour variations quantitatively.

This colorimetric analysis revealed that the incubation at 42 °C does not greatly influence the brightness (L*) of the samples considered,

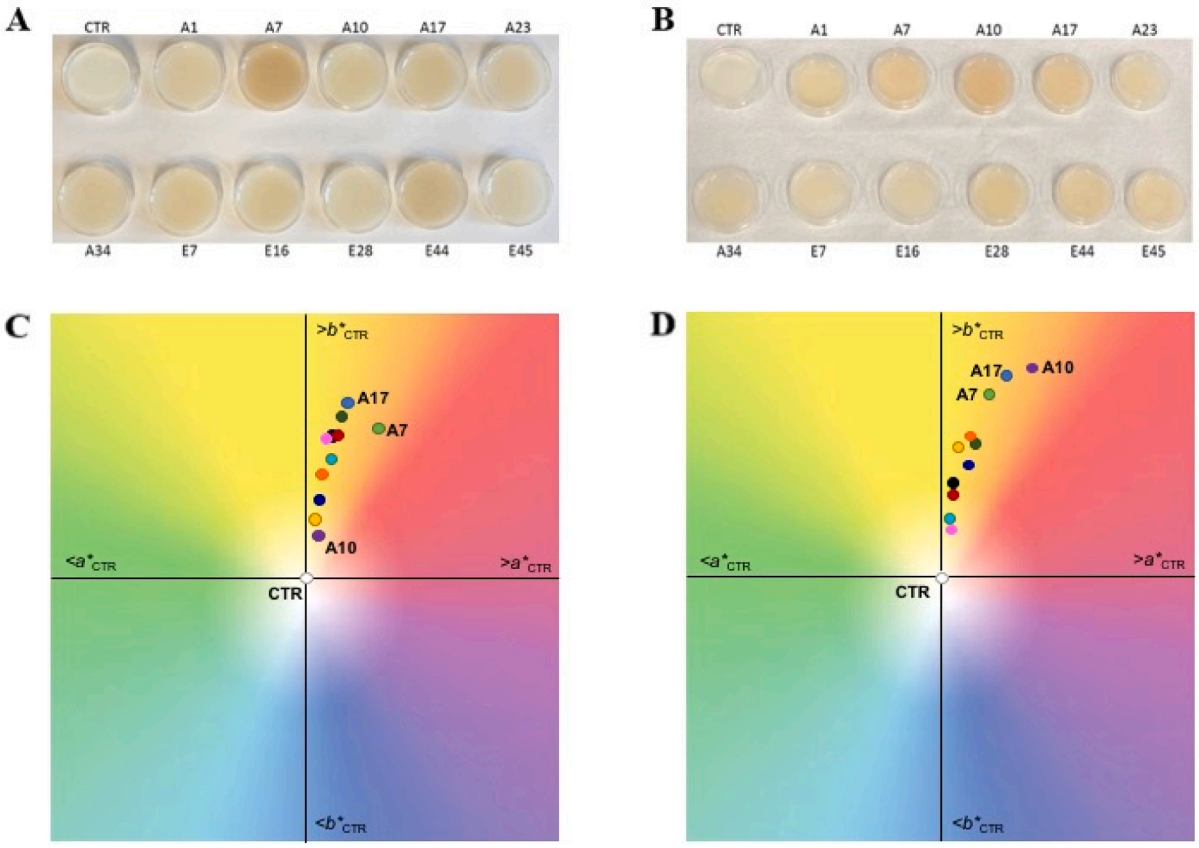

Fig. 1. Appearance of plates inoculated with tested strains (namely CTR, A1, A7, A10, A17, A23, A34, E7, E16, E28, E44, E45) after incubation at 42 °C (A) and further incubated at 16 °C (B). Graphical representation of colorimetric coordinates (a* and b*) of RCWM (rennet casein whey medium) inoculated with the different *L. helveticus* strains after incubation at 42 °C (C) and at 16 °C (D). In graphs C and D, the axes represent increasing and decreasing values of a* and b* when compared with the colorimetric coordinates of the CTR (a^*_{CTR} and b^*_{CTR}), in the center of the CIELAB coordinates graph. Legend of the graph: CTR •; A7 •; A17 •; A10 •; A23 •; A34 •; E7 •; E16 •; E28 •; E44 •; E45 •. CTR •: negative control tube (not inoculated with *L. helveticus*).

except for the darkness of A7, A10 and A1 (supplementary Table 1). The growth of strains in RCWM caused a significant increase of a* values in all tubes, reaching the highest value in sample A7 (3.23 ± 0.18) (Fig. 1 C). This latter showed a higher red coloration than the other samples, characterized by negative or close to 0 a* values. All samples showed a strongly marked yellow-orange coloration (b*) compared with the control (4.76 ± 0.04), which is the typical straw-yellow coloration of uninoculated RCWM after its incubation at 42 °C.

Furthermore, strain A7 had the smallest hue angle, h (°), being 78.78 ± 0.34, meaning that its colour was closer to pure red than the others, showing all have h-values higher than 87 (bringing them closer to yellow coloration) (supplementary Table 2). Also considering the C* values, the strains A7, A10 and A17 exhibited shades of orange and red (supplementary Table 2).

Subsequently, some samples noticed changes in trichromatic coordinates after incubating at 16 °C (Fig. 1 D). At this incubation temperature, brightness (L*) values were not highly affected except for A34, E16, E7 and A10 strains that showed L* values lower than 70, being darker than the control. In addition, A10, A17, and A7 strains were the only ones showing positive a* coordinates. All the other samples were characterized by negative values for a* parameter, thus leaning towards the green color. The samples under investigation also showed an increase in the b* coordinates compared to the control sample; in this regard, the yellow coloration followed the order A7 < A17 < A10 strains. These latter also showed a more pronounced browning process, confirmed by the highest a* and b* values (Supplementary Figs. 1 and 2, respectively), and the smallest hue angles (lower than 90), thus explaining a greater closeness to pure red coloration. This trend was also confirmed by inspecting the C* coordinates of these strains (supplementary Table 2), corresponding to a greater colour vivacity and saturation.

Regarding the ΔE* parameter (supplementary Table 3), a colour variation could be detected for all strains, presenting values always greater than 5, meaning a variation that can be perceived also by the observer. Finally, to better understand the effect of the different temperatures on the variation of colour, the ΔE* was also calculated for each sample between 42 °C and 16 °C (supplementary Table 2). Overall, the E44 strain changed its colour after the second incubation, but this variation was noticeable only for experienced observers (ΔE* lower than 2). On the other hand, all the other strains showed a more pronounced colour difference, with the A10 strain being the one where this deviation was more evident (i.e., as outlined by the highest ΔE* value).

3.3. Methylglyoxal production from L. helveticus strains in whey and RCW media

To discriminate strains for their MG production, a targeted analytical approach based on UHPLC-HRMS was used to quantify this metabolite on whey and RCWM after the growth of each strain at 42 °C for 72 h. The results of methylglyoxal quantification are reported in Table 1. Starter cultures typically used in cheese production (e.g., *L. helveticus*) were shown to produce 0.5 up to 2.37 μg/mL of MG in MRS medium modified to simulate cheese during early ripening (McDonald, 1992). However, our isolates did not grow in a synthetic medium, thus hampering the comparison with previous studies. Furthermore, the data in the bibliography concerning the amount of MG produced by *L. helveticus* were obtained with analytical methods different from that used in this work. In this regard, we adopted for the first time an analytical protocol based on the targeted quantification of MG by high-resolution mass spectrometry, following derivatization with 4-PDA, which has been previously reported to provide high responsiveness when dealing with ESI-MS detection methods (Fritzsche et al., 2018). Moreover, the accumulation of MG was higher in RCWM than in whey (Table 1), even if the values obtained are included in the range described by McDonald (1992). Interestingly, as detailed in Table 1, the A7 strain showed the highest MG production in RCWM, compared to the remaining strains. The MG amounts detected in the two media (RCWM *vs* WM) could be due to both differences in their chemical composition and different availability of precursor compounds accelerating the non-enzymatic browning. The increased complexity of RCWM could affect strain growth and likely the metabolic pathways leading to MG production. Indeed, the role of oligopeptides and amino acids in the formation of AGE products associated with the production of MG has been previously described (Scalone et al., 2015).

3.4. Evaluation of autolysis of the different L. helveticus strains

To assess the autolytic capacity of our strains, we performed plate counts for each sampling time, i.e., 24, 48 and 72 h for both 42 °C and 16 °C incubation. The results are shown in Fig. 2A. As expected, we found different survival between the strains. For some strains (A10, E16, E28, E44 and E45), the mortality at the end of the experiment (72 h at 16 °C) appeared to be 100 %. While for some, and in particular strain A7, plate counts showed high survival.

Without any presumption of correlating the autolysis obtained in our conditions with that which would be obtained in cheese, we quantified the amount of the bacterial DNA released during the growth phases of our strains. The purpose of this quantification was to evaluate the contribution of autolysis in the formation of some compounds associated with discoloration. The results are presented as Log number of genomes per mL in Fig. 2B. As shown, there was an increase in free DNA from the first 24 h at 42 °C. The amount of DNA released in the culture medium increased progressively in all strains. Instead, at the last sampling (16 °C, 72 h) there was a reduction in the amount of DNA detected. This reduction could be due to a degradation of free DNA as reported by Treimo et al. 2006. Indeed, a balance is established between released and degraded DNA. In the latest sampling, however, it appears that the degraded DNA far exceeds that released by the cells in autolysis. The concentration of free DNA recorded seems to be very similar for the different strains tested, with the exception of isolates A1 and A7. Strains A17, A23, E7 and E44 seem to reach the highest concentration starting at 72 h at 42 °C. Interestingly, however, the highest amounts of free DNA were generally detectable close to 72 h of incubation at 42 °C. We consider these data as preliminary and further investigations are necessary.

3.5. Comprehensive characterization of the chemical changes induced by the different L. helveticus strains

In this work, the untargeted metabolomics-based approach allowed to putatively annotate 4033 mass features (with the level 2 of confidence in annotation, according to the COSMOS metabolomics standard initiative), with 100 metabolites confirmed by MS/MS, using the FooDB database as a reference. The dataset containing all the information related to the annotation step (such as relative abundance values, composite mass spectra, and additional information) can be found in supplementary Table 4 (data sheet b.). To reduce the complexity of the omics dataset, we extrapolated some compounds of interest according to the browning process previously described and observed in cheese by some research groups (Divine et al., 2012; Divine and Rankin, 2013; Gandhi et al., 2019, 2018). In this regard, we considered several classes of metabolites naturally involved in the browning process, namely amino acids, pyrazines, beta-carbolines, furans and furanones, pyrroles, pyridine derivatives, oligopeptides (mainly dipeptides), followed by some compounds recognized as intermediates in the glycolytic pathway.

To naively group within the different incubation conditions (42 °C and 16 °C), two unsupervised hierarchical clustering analyses (HCA) were carried out, hence considering the only similarities/dissimilarities in their chemical profiles according to Euclidean distances. The corresponding heat maps are reported in supplementary Fig. 3 for 42 °C and 16 °C, respectively, providing a separation pattern based on two main sample groups (i.e., cluster 1 and cluster 2). as far as the heat map at

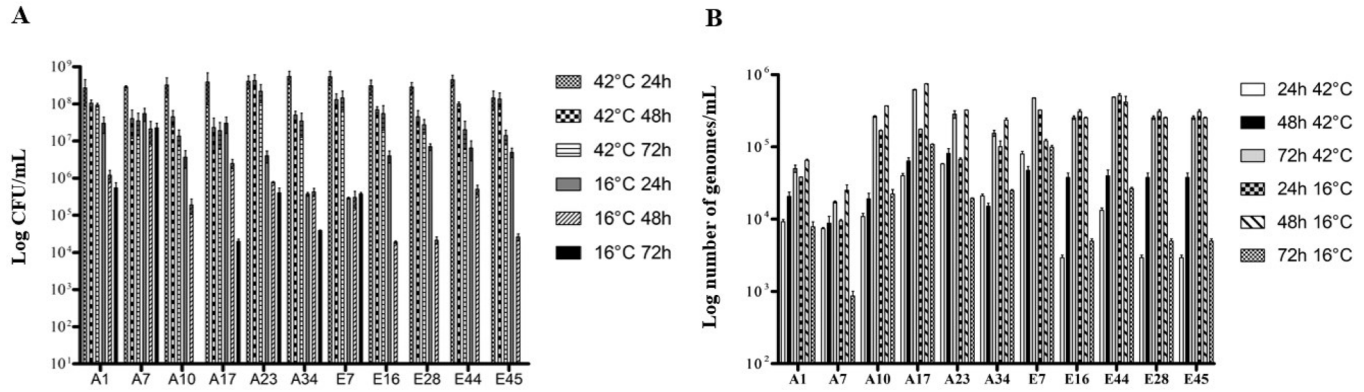

Fig. 2. Evaluation of autolysis capability of the isolated *L. helveticus* strains. A) Values related to Log CFU/mL for each *L. helveticus* strains at different sampling time (24, 48, 72 h) for both incubations (42 °C and 16 °C), and B) quantification of the amount of the bacterial DNA (as Log number of genomes/mL) released during the growth phases.

42 °C is concerned (supplementary Fig. 3A), the cluster 1 consisted in two main subclusters, including on one side E16, A7, and A1 strains, and on the other side E44, E28, E45, and A23. Moreover, cluster 2 consisted of the CTR sample (showing a more exclusive chemical profile), together with E7, A10, A34, and A17 strains. Regarding supplementary Fig. 3B (the heat map at 16 °C), cluster 1 consisted of A1, A10, A7, A17, and E7 strains, while cluster 2 was characterized by the CTR sample and the remaining strains (E16, E28, E44, E45, A23, and A34). The sample grouping observed at 42 °C is related to strain-dependent properties since cells are metabolically active. In comparison, the grouping at 16 °C is likely resulted from potential reactions promoted by active enzymes and reactive compounds accumulated in the medium, such as MG.

3.6. Screening of L. helveticus strains involved in browning by untargeted metabolomics

As the next step, we used untargeted metabolomics profiles to specifically investigate the most predictive metabolites as a function of the browning discoloration observed. Therefore, multivariate statistics based on supervised OPLS-DA were carried out to build up two prediction models using a combination of metabolomics- and colorimetric-based data (Fig. 1 A and B; supplementary Table 1). The resulting OPLS-DA score plots are reported in Fig. 2 A and 2B for 42 °C and 16 °C, respectively. The corresponding discriminant metabolites correlated to the browning process together with cross-validation ANOVA ($p < 0.05$), permutation testing plots (number of random replications: 100; to exclude overfitting) and the Hotelling's T2 range test (to evaluate strong and suspect outliers in prediction) can be found in supplementary Table 4 (data sheet c.).

Overall, looking at the OPLS-DA score plot in Fig. 3A, we found a clear separation along the orthogonal latent vector between those strains having positive a* values (A7, A17, and E44) and all the other remaining strains (including the CTR sample). It was interesting to notice that the prediction model was characterized by a good robustness, being the goodness-of-fitting (R^2Y) equal to 0.99 and the goodness-of-prediction (Q^2) equal to 0.61. The following variables' importance in projection approach (VIP) allowed us to extrapolate the most discriminant compounds (metabolites/intermediates) involved in the browning. As reported in supplementary Table 4 (data sheet d.), 86 compounds were associated with browning possessed VIP scores > 1, thus outlining a good discrimination ability. Among these metabolites, we found markers of proteolysis like several peptides (62 compounds; mostly di-peptides) and 9 amino acids, followed by 7 pyrazines, 4 furans and furanones, 2 glycolysis-related compounds (i.e., pyruvate and S-Lactoylglutathione), and 2 additional small-molecular-weight metabolites.

Looking at the discriminant metabolites at 42 °C incubation (supplementary Table 4), the highest prediction scores were recorded for three metabolites (Table 2), all being markers of the "browning group", namely 5-methyl-3(2H)-furanone (VIP score = 2.62; $Log_2FC = 0.76$), S-Lactoylglutathione (VIP score = 2.35; $Log_2FC = 2.36$), and 2,6-diethyl-3,5-dimethylpyrazine (VIP score = 2.05; Log_2FC value = 0.73). Besides, the AUC values (from ROC curves) allowed to validate the discriminant potential of these 3 discriminant marker compounds, revealing AUC values ranging from 0.75 and 0.87 (Table 2 and supplementary Fig. 4).

5-methyl-3(2H)-furanone belongs to the class of furans and furanones and this class of metabolites has been previously described in

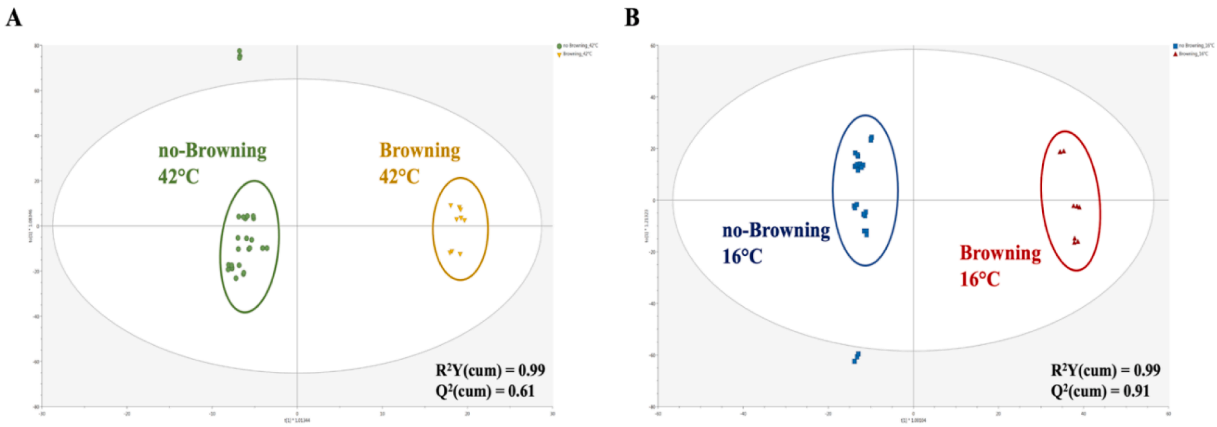

Fig. 3. Supervised OPLS-DA discriminant models considering the metabolomic profiles of *L. helveticus* strains incubated in RCWM (rennet casein whey medium) at both 42 °C (A) and 16 °C (B). The goodness of fitting (R^2Y) and goodness of prediction (Q^2) parameters are also provided.

Table 2
Most significant and discriminant VIP marker compounds considering both 42 °C and 16 °C incubation temperatures. Abbreviations: AUC (area under the curve), VIP (variable's importance in projection), ROC (receiver operating characteristics).

VIP marker 42 °C	AUC (ROC curve)	VIP score (OPLS-DA)	*p*-value (ANOVA)	Log_2FC (Fold-Change)
S-Lactoylglutathione	0.75	2.35	3.4×10^{-3}	2.36
5-methyl-3(2H)-furanone	0.87	2.62	2.5×10^{-4}	0.76
2,6-diethyl-3,5-dimethylpyrazine	0.81	2.05	2.0×10^{-3}	0.73
VIP marker 16 °C	**AUC (ROC curve)**	**VIP score (OPLS-DA)**	***p*-value (ANOVA)**	**Log_2FC (Fold-Change)**
Glutamyl-threonine	0.99	1.99	4.2×10^{-10}	3.08
Leucyl-asparagine	1.00	2.08	3.6×10^{-12}	2.04
Na-Formyl-1-methyl-β-carboline	0.66	1.04	2.9×10^{-2}	0.77
L-Lysine	0.95	1.85	8.8×10^{-8}	1.46
2,3,5-trimethyl-6-[4-(methylthio)butyl] pyrazine	1.00	1.82	4.6×10^{-8}	4.92

relation to LAB strains (such as *L. helveticus*) exposed to stress conditions (such as oxidative and/or heat stress) (Ndagijimana et al., 2006). Therefore, it can be postulated that the production of 5-methyl-3(2H)-furanone was triggered by the methylglyoxal accumulation in the media, and thus directly correlated with the browning process under investigation. Furthermore, we found an extremely high discrimination power for the thiol-dependent glyoxalase-intermediate S-Lactoylglutathione; this compound is an essential detoxification agent to fight the accumulation and toxicity of the unstable MG (Suttisansanee and Honek, 2011). Therefore, the prediction model built confirmed the existence of multiple biochemical routes that are directly correlated with the browning observed. Last but not least, it is important to mention the compound 2,6-diethyl-3,5-dimethylpyrazine as a discriminant marker. Historically, the correlation between pyrazines and browning discoloration was first reported by Divine and co-authors (2012), revealing (using a GC–MS approach) the presence of six pyrazines in the volatile fraction of Parmesan cheese (experiencing browning defect) stored at low temperature. In particular, the synthesis of pyrazines was proposed to result from the spontaneous condensation of aminoacetone (downstream formed by the Strecker degradation of amino acids with methylglyoxal). Therefore, our findings corroborate the existing scientific literature data, revealing that additional pyrazines in the RCWM are directly involved in browning and possessing a high discrimination degree (such as 3-methylpyrrolo[1,2-a]pyrazine, 3,5-Diethyl-2-methylpyrazine, and 2-acetyl-3-ethylpyrazine; supplementary Table 4). Future works based on the targeted analysis of these compounds and their absolute quantification appear to be of great interest in developing rapid and effective screening methods for these compounds involved in browning discoloration.

As far as the browning discoloration at 16 °C is concerned, we carried out an additional OPLS-DA prediction model, assigning each strain to "browning" *vs* "no Browning" groups according to the colorimetric measurements. The second OPLS-DA score plot is reported in Fig. 3B. Interestingly, we found a good separation along the orthogonal components between three strains classified as "browning", namely A7, A17 and A10 compared to the remaining strains. Also, the parameters associated with the goodness of fitting and prediction were higher when compared to the previous model, recording a $Q^2 = 0.914$. Furthermore, a higher number of discriminant compounds potentially involved in the browning process could be extrapolated (152), with a great abundance of peptides (118 compounds) and other compounds (such as amino acids, furans and furanones, glycolysis-intermediates, beta-carboline derivatives, and pyrazines) (supplementary Table 4, data sheet e.). In supplementary Table 4 (data sheet f.), a Venn diagram revealed that the combination of the two different incubation temperatures promoted the up/down-accumulation of exclusive metabolites (92 compounds), when compared with only incubation at 42 °C (only 26 exclusive compounds), with 60 common discriminant metabolites (33.7 %) identified. As previously stated, we could suppose that the differences in discriminant metabolites detected at 42 °C *vs*. 16 °C have a different origin. Indeed, during the incubation at 42 °C, bacterial cells hydrolysed casein to support their growth while at the end of the stationary phase they can undergo lysis and release enzymes in the medium, as occurs during cheese ripening (Lazzi et al., 2016; Gatti et al., 2014). Under our conditions, we can assume a contribution of autolysis in the formation of certain compounds, as our data show a release of DNA already at 72 °C incubation at 42 °C. Thus, the contribution of enzymes released by autolysis may be more important for some strains such as A10, A17, A23 and E44 compared to strains A1 and A7 which showed limited lysis.

Looking at the discriminant compounds of the second OPLS-DA model built, we found a lower discrimination ability for pyrazines, with only 2 out of 5 discriminant compounds possessing a VIP score > 1, namely 2,3,5-trimethyl-6-[4-(methylthio)butyl]pyrazine (VIP score = 1.82) and 3-methylpyrrolo[1,2-a]pyrazine (VIP score = 1.35). Accordingly, among the best discriminant compounds of this model, we found mainly 11 peptides and amino acids with VIP scores > 1.80. Going into detail, the best discriminant markers were 2 dipeptides, namely leucyl-asparagine (VIP score = 2.08; $Log_2FC = 2.04$) and glutamyl-threonine (VIP score = 1.99; $Log_2FC = 3.08$) (Table 2). Besides, the AUC values (from ROC curves) allowed to validate the discriminant potential of these 5 discriminant marker compounds, revealing AUC values ranging from 0.66 and 1.00 (Table 2 and supplementary Fig. 4). The high discrimination ability observed for dipeptides and amino acids (such as lysine, Table 2) after the incubation at 16 °C is compatible with the proteolytic activity of *L. helveticus* (also highlighted in supplementary Table 4 by inspecting the comparisons 42 °C *vs* 16 °C for most of the strains under investigation). In fact, *L. helveticus* is considered one of the most efficient proteolytic strains within the microbiota of cheese, and a primary producer of various bioactive peptides from caseins (Beganović et al., 2013). Looking at the scientific literature, Scalone et al. (2015) studied the influence of free amino acids, oligopeptides, and polypeptides on the formation of pyrazines in a whey proteins-based model system. These authors evaluated if the compounds responsible for pyrazine generation were the free amino acids arising from whey proteins hydrolysis, the peptide fraction, or both. Under dry heating conditions, model systems containing hydrolysed whey proteins and glucose led to the formation of the highest amounts of pyrazines. On the other hand, the models containing native whey protein and glucose showed a significantly lower production of pyrazines than samples with hydrolysed whey. It is important to mention that the whey used likely contained peptides and free amino acids coming from casein hydrolysis, initially present in milk and/or generated during whey manufacture, and all these factor could have contributed to the browning observed.

Among the exclusive discriminant compounds of the incubation at 16 °C, we found four β-carboline derivatives, namely Na-Formyl-1-methyl-β-carboline, L-1,2,3,4-Tetrahydro-β-carboline-3-carboxylic acid, 1-(1,2,3,4,5-Pentahydroxypent-1-yl)-1,2,3,4-tetrahydro-β-carboline-3-carboxylate, and (1xi,3S)-1,2,3,4-Tetrahydro-1-methyl-β-carboline-1,3-dicarboxylic acid. Accordingly, in a previous work by Gandhi et al. (2019), the accumulation of heterocyclic amines (including β-carboline derivatives) arising from MG synthase (*mgsA*) was reported. The authors demonstrated that the microbial production of MG can lead to the formation of late-stage Maillard reaction products (such as beta-carbolines), thus effectively circumventing the thermal requirement of the early- and intermediate-stages of Maillard reaction. In our experimental conditions, Na-Formyl-1-methyl-b-carboline was the most discriminant beta-carboline derivative (VIP score = 1.04; Log_2FC = 0.77, a marker of the "browning group"). Overall, such findings about

the discriminant power of beta-carboline derivatives towards browning events at 16 °C is in accordance with the ability of MG to accelerate the formation of Maillard-intermediates and its final products in the absence of high temperatures.

According to the few scientific works to date available on the browning process in cheese or cheese-based models, a higher production of methylglyoxal by LAB (a potentially toxic and reactive metabolite) can be correlated to the activation of several detoxification pathways involving the glyoxalase system (Gandhi et al., 2019), together with the ability of strains to convert methylglyoxal into 1,2-propanediol and/or to produce the so-called advanced glycation end products (deriving from fatty acid oxidation, protein catabolism, and Maillard reaction) (Gandhi et al., 2019).

In this framework, it is known that pyrazine formation can occur from the nucleophilic addition to methylglyoxal by primary amines to form aminoacetone, whereby condensation can form nitrogenous cyclic compounds with various side chains. Under our experimental conditions, we found an up-accumulation of total pyrazines following the incubation of the A7 strain at 42 °C and 16 °C (Fig. 4A). In this regard, we recorded Log_2FC values against the A7 strain ranging from 0.27 (for the A23 strain) up to 1.19 (for the E16 strain) (supplementary Table 4). Interestingly, the same up accumulation recorded in terms of Log_2FC values for total pyrazines was found in the A7 strain following the incubation at 16 °C, obtaining values from 0.99 (for the A17 strain) up to 2.13 (for the A34 strain). In addition, as reported in Fig. 4B, the reduction of the peptides and dipeptides at 16 °C seems to correlate with a higher production of pyrazines, which was true mainly for the A7, E7, E16 and E28 strains. On the other hand, the cumulative profile of amino acids at 16 °C (Fig. 4C) seems to be related more to the presence of active proteolytic enzymes than pyrazines' production. Therefore, it is possible to speculate about preferential detoxification pathways (mainly involving the A7 strain), which contribute to the production of pyrazines and are directly involved in the browning process (Divine et al., 2012).

As previously stated, most lactic acid bacteria (including *L. helveticus*, *Levilactobacillus brevis*, *Lacticaseibacillus casei*, *Limosilactobacillus fermentum*, *Lactiplantibacillus plantarum*, *Limosilactobacillus reuteri*, *Lacticaseibacillus rhamnosus*, and *Latilactobacillus sakei*) metabolized MG to either acetol or 1,2-propanediol, representing partially and fully reduced forms of MG, respectively (Gandhi et al., 2018). Under our experimental conditions, we corroborated the role of this detoxification route, obtaining the highest relative abundance values of 1,2-propanediol following the incubation of A7 strain at 42 °C and recording Log_2FC values against A7 strain in the range 0.81 (for E16 strain) up to 2.16 (for A1 strain) (supplementary Table 4). Interestingly, the metabolomics dataset also revealed the presence of the glyoxalase-pathway intermediate S-Lactoylglutathione (Fig. 4D). Accordingly, a well-studied detoxification adduct is the thiol-dependent glyoxalase pathway, which protects against MG accumulation and as an energy-futile glycolytic bypass (Suttisansanee and Honek, 2011). The pathway consists of a 2-step reaction involving the thiol group of glutathione to form the important intermediate S-Lactoylglutathione and then the end-product lactic acid. In this work, the highest accumulation of S-Lactoylglutathione was found for the A7 strain, the one producing more total pyrazines after both incubation conditions. This is in accordance with the highest production of MG in the RCWM by the A7 strain, showing the highest residual accumulation (Table 1) and, therefore, likely being the most active strain in terms of MG detoxification.

Evaluating a time-course on the production of MG and/or correlated detoxification metabolites is a rather challenging task. Indeed, the metabolomics findings revealed that the browning phenomena are complex, with combinatory conjugations and a multi-level crosstalk of

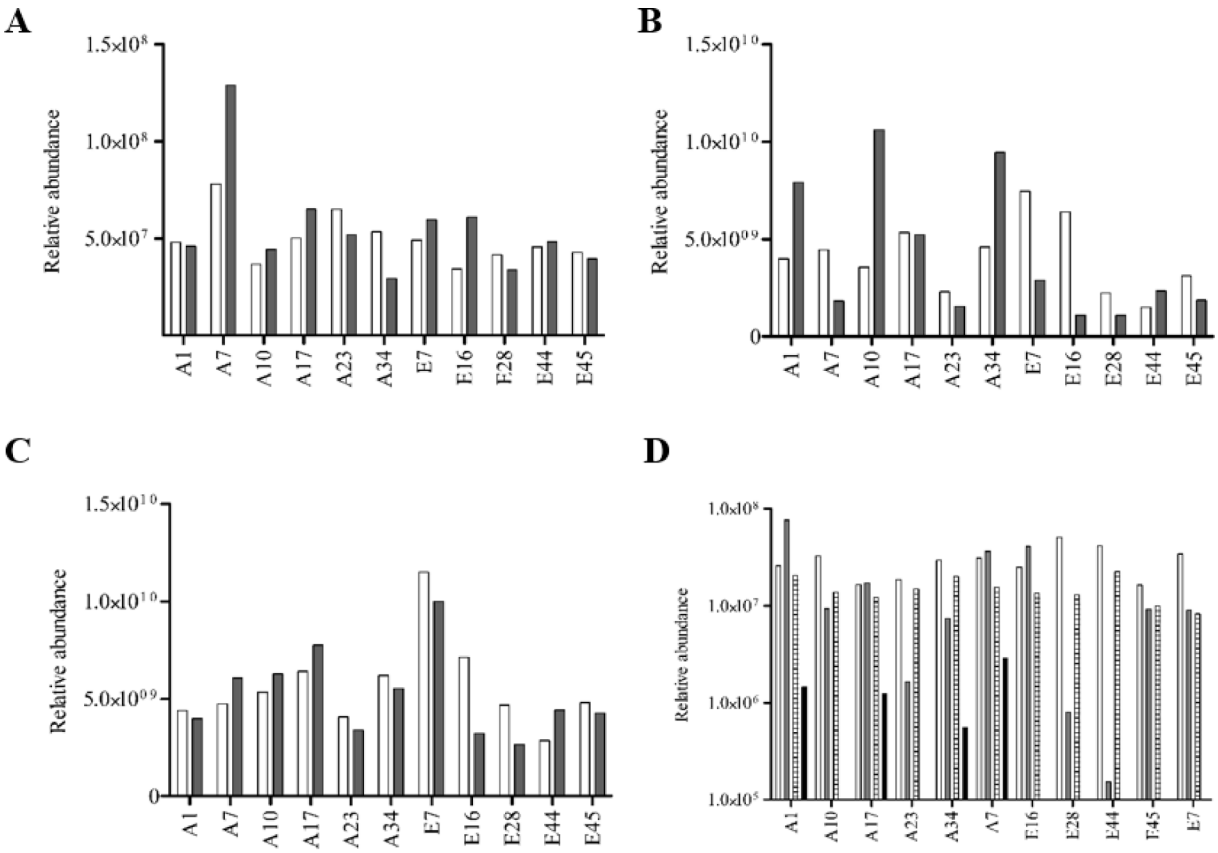

Fig. 4. Total amount of metabolites naturally involved in browning process, such as pyrazines (A), oligopeptides (B), amino acids (C) considering the incubation at 42 °C (white bar) and 16 °C (black bar). Concerning the glycolytic pathway intermediates (D) data refer to samples obtained at 42 °C. In this figure the average relative abundance of dihydroxyacetone phosphate (white bar), pyruvate (grey bar), lactic acid (striped bar) and S-Lactoylglutathione (black bar) is represented.

different biochemical processes involved, some of which are essential to protect bacteria from MG toxicity. Within this framework, the use of untargeted metabolomics allows a more comprehensive evaluation of the processes underlying browning in cheeses. Nonetheless, in this work, we provided evidence that the different *L. helveticus* strains can metabolize MG by multiple and preferential biochemical routes, such as both thiol-dependent (involving glutathione intermediates) and thiol-independent (such as those based on AGE-products, pyrazines, and/or 1,2-propanediol) manner.

4. Conclusions

In this work, we demonstrated that using RCWM allowed reliable discrimination of *L. helveticus* strains based on their potential in triggering browning discoloration. This approach is rapid and easy to perform, and the results are reliable. First, the test performed to evaluate colour changes are repeatable, and these variations are easily visible for the strain more involved in this process. For the other strains, whose effects are not appreciable with the simple visual analysis, the colorimetric analysis overcomes this issue. Furthermore, the MG content and the different metabolites detected in the synthetic medium after the growth of bacteria supported the occurrence of browning. Indeed, metabolomics identified compounds, such as pyrazines and β-carbolines, already reported to be associated with the browning process in cheeses. Noteworthy, our data refer to only four strains out of 11 having a browning potential, hence demonstrating this is a strain-specific feature. Moreover, our protocol provided early evidence about the browning defect using an *"in vitro"* system, a screening tool that does not involve cheese making. This point is of primary relevance from a dairy industry perspective. Additionally, the multivariate statistical analysis of metabolomics-based data showed some discriminant compounds potentially associated with the presence of a thiol-independent reduction system. Therefore, although our data indicate a good capability of the RCWM to select and discriminate strains potentially involved in browning discoloration, it should be emphasized that during the production of cheeses, the technology and the interactions between bacteria can modify their behaviour. This could explain the sporadic appearance of browning since it is a complex balance between environmental, microbiological, and technological factors.

CRediT authorship contribution statement

Sofia Galimberti: Methodology, Formal analysis, Investigation, Writing – original draft, Visualization. **Gabriele Rocchetti:** Methodology, Formal analysis, Investigation, Writing – original draft, Writing – review & editing, Visualization. **Francesca Di Rico:** Formal analysis. **Chiara Rossetti:** Methodology, Formal analysis, Investigation, Writing – original draft, Visualization. **Alessandra Fontana:** Writing – review & editing. **Luigi Lucini:** Supervision, Methodology, Investigation, Writing – review & editing. **Maria Luisa Callegari:** Conceptualization, Supervision, Methodology, Formal analysis, Investigation, Writing – original draft, Writing – review & editing, Visualization.

Declaration of Competing Interest

The authors declare that they have no known competing financial interests or personal relationships that could have appeared to influence the work reported in this paper.

Data availability

Data will be made available on request.

Acknowledgements

The authors wish to thank the Cremona Agri-food technologies project (CRAFT) funded by Fondazione Cariplo and Regione Lombardia and the "Romeo ed Enrica Invernizzi" foundation for the kind support to the metabolomics facility at the Faculty of Food, Agriculture and Environmental Science, Università Cattolica del Sacro Cuore. S.G., F.D.R., and C.R. were recipient of a Ph.D. fellowship (AgriSystem) from the Università Cattolica del Sacro Cuore (Piacenza, Italy). We are deeply grateful to Ernesto Brambilla and Guillermo Duserm Garrido, laboratory technicians of the Department for Sustainable Food Process, for their valuable technical assistance.

Appendix A. Supplementary material

Supplementary data to this article can be found online at https://doi.org/10.1016/j.foodres.2023.113644.

References

Ackerman, R. S., Cozzarelli, N. R., & Epstein, W. (1974). Accumulation of toxic concentrations of methylglyoxal by wild type *Escherichia coli* K12. *Journal of Bacteriology, 119*, 357–362. https://doi.org/10.1128/jb.119.2.357-362.1974

Beganović, J., Kos, B.Ž., Leboš Pavunc, A., Uroić, K., Džidara, P., & Šušković, J. (2013). Proteolytic activity of probiotic strain *Lactobacillus helveticus* M92. *Anaerobe, 20*, 58–64. https://doi.org/10.1016/j.anaerobe.2013.02.004

Biró, B., Fodor, R., Szedljak, I., Pásztor-Huszár, K., & Gere, A. (2019). Buckwheat-pasta enriched with silkworm powder: Technological analysis and sensory evaluation. *LWT, 116*, Article 108542. https://doi.org/10.1016/j.lwt.2019.108542

Blaženović, I., Kind, T., Ji, J., & Fiehn, O. (2018). Software tools and approaches for compound identification of LC-MS/MS data in metabolomics. *Metabolites, 8*, 31. https://doi.org/10.3390/metabo8020031

Bottazzi, V., Cappa, F., Scolari, G., & Parisi, M. (2000). Occurring of pink discolouration in Grana cheese made with one-strain starter culture. *Scienza e Tecnica Lattiero Casearia, 51*, 67–74.

Cocconcelli, P. S., Parisi, M. G., Senini, L., & Bottazzi, V. (1997). Use of RAPD and 16S rDNA sequencing for the study of *Lactobacillus* population dynamics in natural whey culture. *Letters in Applied Microbiology, 25*, 8–12. https://doi.org/10.1046/j.1472-765X.1997.00061.x

Divine, R. D., & Rankin, S. A. (2013). Short communication: Reducing agents attenuate methylglyoxal-based browning in parmesan cheese. *Journal of Dairy Science, 96*, 6242–6247. https://doi.org/10.3168/jds.2013-6890

Divine, R. D., Sommer, D., Lopez-Hernandez, A., & Rankin, S. A. (2012). Short communication: Evidence for methylglyoxal-mediated browning of Parmesan cheese during low temperature storage. *Journal of Dairy Science, 95*, 2347–2354. https://doi.org/10.3168/jds.2011-4828

Ferguson, G. P., Tötemeyer, S., MacLean, M. J., & Booth, I. R. (1998). Methylglyoxal production in bacteria: Suicide or survival? *Archives of Microbiology, 170*(4), 209–218.

Fritzsche, S., Billig, S., Rynek, R., Abburi, R., Tarakhovskaya, E., Leuner, O., … Birkemeyer, C. (2018). Derivatization of methylglyoxal for LC-ESI-MS analysis—stability and relative sensitivity of different derivatives. *Molecules, 23*. https://doi.org/10.3390/molecules23112994

Gandhi, N. N., Barrett-Wilt, G., Steele, J. L., & Rankin, S. A. (2019). *Lactobacillus casei* expressing methylglyoxal synthase causes browning and heterocyclic amine formation in Parmesan cheese extract. *Journal of Dairy Science, 102*, 100–112. https://doi.org/10.3168/jds.2018-15042

Gandhi, N. N., Cobra, P. F., Steele, J. L., Markley, J. L., & Rankin, S. A. (2018). Lactobacillus demonstrate thiol-independent metabolism of methylglyoxal: Implications toward browning prevention in Parmesan cheese. *Journal of Dairy Science, 101*, 968–978. https://doi.org/10.3168/jds.2017-13577

Gatti, M., Bottari, B., Lazzi, C., Neviani, E., & Mucchetti, G. (2014). Invited review: Microbial evolution in raw-milk, long-ripened cheeses produced using undefined natural whey starters. *Journal of Dairy Science, 97*(2), 573–591. https://doi.org/10.3168/jds.2013-7187

Giraffa, G. (2021). The microbiota of Grana Padano cheese. *A review. Foods, 10*, 2632. https://doi.org/10.3390/foods10112632

Hatti-Kaul, R., Chen, L., Dishisha, T., & Enshasy, H. E. (2018). Lactic acid bacteria: From starter cultures to producers of chemicals. *FEMS Microbiology Letters, 365*(20). https://doi.org/10.1093/femsle/fny213

Hernández, B., Sáenz, C., Alberdi, C., & Diñeiro, J. M. (2016). CIELAB color coordinates versus relative proportions of myoglobin redox forms in the description of fresh meat appearance. *Journal of Food Science and Technology, 53*, 4159–4167. https://doi.org/10.1007/s13197-016-2394-6

Lazzi, C., Povolo, M., Locci, F., Bernini, V., Neviani, E., & Gatti, M. (2016). Can the development and autolysis of lactic acid bacteria influence the cheese volatile fraction? The case of Grana Padano. *International Journal of Food Microbiology, 233*, 20–28. https://doi.org/10.1016/j.ijfoodmicro.2016.06.009

Lee, C., & Park, C. (2017). Bacterial responses to glyoxal and methylglyoxal: Reactive electrophilic species. *International Journal of Molecular Science, 18*(1), 169. https://doi.org/10.3390/ijms18010169

Li, M., Shen, M., Lu, J., Yang, J., Huang, Y., Liu, L., … Xie, M. (2022). Maillard reaction harmful products in dairy products: Formation, occurrence, analysis, and mitigation

strategies. *Food Research International, 151*, Article 110839. https://doi.org/10.1016/j.foodres.2021.110839

McDonald, S.T. (1992). Role of alpha-dicarbonyl compounds produced by lactic acid bacteria on the flavor and color of cheeses - ProQuest.

Miragoli, F., Patrone, V., Romaniello, F., Rebecchi, A., & Callegari, M. L. (2020). Development of an S-layer gene-based PCR-DGGE assay for monitoring dominant *Lactobacillus helveticus* strains in natural whey starters of Grana Padano cheese. *Food Microbiology, 89*. https://doi.org/10.1016/j.fm.2020.103457

Moser, A., Berthoud, H., Eugster, E., Meile, L., & Irmler, S. (2017). Detection and enumeration of *Lactobacillus helveticus* in dairy products. *International Dairy Journaal, 68*, 52–59. https://doi.org/10.1016/j.idairyj.2016.12.007

Moser, A., Wüthrich, D., Bruggmann, R., Eugster-Meier, E., Meile, L., & Irmler, S. (2017). Amplicon Sequencing of the slpH Locus Permits Culture-Independent Strain Typing of *Lactobacillus helveticus* in Dairy Products. *Frontiers in Microbiology, 8*, 1380. https://doi.org/10.3389/fmicb.2017.01380

Ndagijimana, M., Vallicelli, M., Cocconcelli, P. S., Cappa, F., Patrignani, F., Lanciotti, R., & Guerzoni, M. E. (2006). Two 2[5H]-furanones as possible signaling molecules in Lactobacillus helveticus. *Applied and Environmental Microbiology, 72*, 6053–6061. https://doi.org/10.1128/AEM.00363-06

Neviani, E., Bottari, B., Lazzi, C., & Gatti, M. (2013). New developments in the study of the microbiota of raw-milk, long-ripened cheeses by molecular methods: The case of Grana Padano and Parmigiano Reggiano. *Frontiers in Microbiology, 4*. https://doi.org/10.3389/fmicb.2013.00036

Pang, Z., Chong, J., Zhou, G., De Lima Morais, D. A., Chang, L., Barrette, M., … Xia, J. (2021). MetaboAnalyst 5.0: Narrowing the gap between raw spectra and functional insights. *Nucleic Acids Research, 49*. https://doi.org/10.1093/nar/gkab382. W388–W396.

Rocchetti, G., Michelini, S., Pizzamiglio, V., Masoero, F., & Lucini, L. (2021). A combined metabolomics and peptidomics approach to discriminate anomalous rind inclusion levels in Parmigiano Reggiano PDO grated hard cheese from different ripening stages. *Food Research International, 149*, Article 110654. https://doi.org/10.1016/j.foodres.2021.110654

Russell, J. B. (1993). Glucose toxicity in Prevotella ruminicola: Methylglyoxal accumulation and its effect on membrane physiology. *Applied and Environmental Microbiology, 59*, 2844–2850. https://doi.org/10.1128/aem.59.9.2844-2850.1993

Scalone, G. L. L., Cucu, T., De Kimpe, N., & De Meulenaer, B. (2015). Influence of free amino acids, oligopeptides, and polypeptides on the formation of pyrazines in Maillard model systems. *Journal of Agricultural and Food Chemistry, 63*, 5364–5372. https://doi.org/10.1021/acs.jafc.5b01129

Senizza, A., Rocchetti, G., Callegari, M. L., Lucini, L., & Morelli, L. (2020). Linoleic acid induces metabolic stress in the intestinal microorganism *Bifidobacterium breve* DSM 20213. *Scientific Reports, 10*, 1–10. https://doi.org/10.1038/s41598-020-62897-w

Suttisansanee, U., & Honek, J. F. (2011). Bacterial glyoxalase enzymes. *Seminars in Cell & Developmental Biology, 22*(3), 285–292. https://doi.org/10.1016/j.semcdb.2011.02.004

This, H. (2015). Solution to Maillard and grilled steak challenge. *Analytical and Bioanalytical Chemistry, 407*, 8173–8174. https://doi.org/10.1007/s00216-015-9001-y

Treimo, J., Vegarud, G., Langsrud, T., & Rudi, K. (2006). Use of DNA quantification to measure growth and autolysis of *Lactococcus* and *Propionibacterium* spp. in mixed populations. *Applied and Environmental Microbiology, 72*(9). https://doi.org/10.1128/AEM.00515-06

Yann, D., Didier, H., Daniel, B., & &,. (2005). Utilisation of the experimental design methodology to reduce browning defects in hard cheeses technology. *Journal of Food Engineering, 68*, 481–490. https://doi.org/10.1016/j.jfoodeng.2004.06.025

Zheng, J., Guo, H., Ou, J., Liu, P., Huang, C., Wang, M., … Xiao, J. (2021). Benefits, deleterious effects and mitigation of methylglyoxal in foods: A critical review. *Trends in Food Science & Technology, 107*, 201–212. https://doi.org/10.1016/j.tifs.2020.10.031